Chinese Chemical Letters 37 (2026) 111714

Contents lists available at ScienceDirect

Chinese Chemical Letters

journal homepage: www.elsevier.com/locate/cclet

Enhanced permeation of berberine by ionic liquids for the treatment of posterior age-related macular degeneration following topical delivery

Xiuyan Li[a,b], Chongjiang Wang[c], Xiwu Zhang[f], Chengcheng Zhao[f], Zhihui Yang[e], Yi Lu[c], Yifan Cai[c], Huiping Lu[a], Hailong Yuan[e,*], Wei Wu[a,c,*], Yikang Dai[d,*]

[a] Center for Medical Research and Innovation, Shanghai Pudong Hospital, Fudan University Pudong Medical Center, Shanghai 201399, China
[b] Key Laboratory of Basic and Application Research of Beiyao, Heilongjiang University of Chinese Medicine, Harbin 150001, China
[c] School of Pharmacy, Fudan University, National Key Laboratory of Advanced Drug Formulations for Overcoming Delivery Barriers and Key Laboratory of Smart Drug Delivery, Ministry of Education, Shanghai 201203, China
[d] Department of Ophthalmology, Renji Hospital, Shanghai Jiao Tong University School of Medicine, Shanghai 200127, China
[e] Department of Pharmacy, Air Force Medical Center, PLA, Air Force Medical University, Beijing 100142, China
[f] Experimental Teaching and Practical Training Center, Heilongjiang University of Chinese Medicine, Harbin 150001, China

ARTICLE INFO

Article history:
Received 25 February 2025
Revised 8 August 2025
Accepted 12 August 2025
Available online 12 August 2025

Keywords:
Age-related macular degeneration
Ionic liquids
Berberine hydrochloride
Pharmacokinetics
Eye drops

ABSTRACT

Age-related macular degeneration (AMD) represents a primary cause of vision loss in the elderly population. Reactive oxygen species (ROS) generation constitutes a pivotal pathogenesis mechanism in AMD. Berberine (BBR) shows therapeutic potential for dry AMD through its ability to mitigate cellular senescence and oxidative stress. However, BBR's low transmembrane permeability severely limits corneal penetration *via* topic administration, creating an urgent need for novel posterior segment delivery strategies. In this study, we employed biocompatible ionic liquids (ILs) to enhance BBR permeation for posterior AMD treatment. Our approach features ocular surface pretreatment with ILs followed by topical administration of BBR solution. Comprehensive *in vitro* and *in vivo* safety assessments confirmed the biocompatibility of monoethanolamine-based IL (Mea-ILs) as ocular penetration enhancers. Trans-monolayer experiments using human corneal epithelial cells (HCECs) demonstrated that ILs enhance paracellular permeability, potentially through tight junction modulation. *In vivo* studies utilizing a sodium iodate-induced dry AMD mouse model revealed that pretreatment with the [monoethanolamine][citric acid] ([Mea][Ci]) IL significantly potentiated BBR's therapeutic efficacy. These findings not only expand pharmaceutical applications of ILs but also establish a safe, efficient strategy for noninvasive dry AMD therapy with BBR. Furthermore, this work provides critical insights for developing advanced penetration enhancers for posterior ocular drug delivery.

© 2026 Published by Elsevier B.V. on behalf of Chinese Chemical Society and Institute of Materia Medica, Chinese Academy of Medical Sciences.

Age-related macular degeneration (AMD) is a leading cause of vision loss in the elderly. Notably, dry AMD comprises 85 %–90 % of all cases [1,2]. The pathogenesis of AMD involves complex interactions among multiple factors and remains incompletely understood. Given the retina's high metabolic demands and the particular susceptibility of retinal pigment epithelium (RPE) cells to oxidative damage, oxidative stress is widely recognized as a risk factor [3]. Since 2023, complement inhibitors such as pegcetacoplan (Syfovre®) and avacincaptad pegol (Izervay®) have been approved for advanced dry AMD. However, these therapies require frequent intravitreal injections (monthly or bimonthly), which carry risks of sight-threatening complications, including irreversible retinal damage.

Berberine (BBR), also known as coptisine, is a quaternary ammonium benzyltetraisoquinoline alkaloid derived from *Coptis chinensis* with diverse pharmacological effects, including anti-inflammatory, antitumor, and immunoregulatory effects [4]. In AMD, reactive oxygen species (ROS) generation constitutes a critical pathogenic mechanism, and RPE cells exhibit particular vulnerability to oxidative damage. BBR mitigates retinal aging by reducing cellular senescence and oxidative stress [5], while also demonstrating efficacy against H_2O_2-induced oxidative injury in D407 cells through modulation of mitochondrial membrane

* Corresponding authors.
E-mail addresses: yhlpharm@126.com (H. Yuan), wuwei@shmu.edu.cn (W. Wu), kangkang56@126.com (Y. Dai).

https://doi.org/10.1016/j.cclet.2025.111714
1001-8417/© 2026 Published by Elsevier B.V. on behalf of Chinese Chemical Society and Institute of Materia Medica, Chinese Academy of Medical Sciences.

potential loss, suppression of caspase-3/7-dependent pathways, reduction of ROS production, and activation of the adenosine 5′-monophosphate-activated protein kinase (AMPK) signaling pathway [6]. Despite these therapeutic benefits, BBR's clinical application for ocular disorders is significantly limited by its low transmembrane permeability [7], which impedes corneal penetration and intraocular distribution following topical administration. Various delivery systems, including liposomes [8], mesoporous silica nanoparticle/thermogel nanocomposites [9], and nanosuspensions [10], have been explored to enhance transcorneal transport. However, the actual penetration enhancement for BBR remains uncertain as existing evaluations predominantly utilized fluorescent probes rather than the compound itself. Furthermore, complex manufacturing requirements and stringent quality control standards hinder the clinical translation and industrial scalability of these technologies. Given that intravitreal injection, the current clinical standard for posterior segment diseases, carries risks of irreversible retinal damage and vision loss [11], the development of novel strategies to improve BBR's ocular permeability represents a research imperative with significant translational potential.

Ionic liquids (ILs), a class of "liquid salts" formed by cationic-anionic pairs, typically exhibit melting points below 100 °C, mostly favorably below room temperature. Recent years have witnessed rapid progress in their biomedical research and applications [12–17]. As emerging chemical penetration enhancers, ILs have demonstrated significant success in facilitating drug permeation across skin and mucosal barriers [16,18–21]. Although ocular drug delivery applications remain nascent, ILs show considerable promise. Betaine- and L-carnitine-based formulations enhanced the solubility, stability, and ocular residence time of diacerein in eye drops [18], while an IL form of pilocarpine achieved a 2-fold increase in corneal permeability [19]. Building upon these advances, this proof-of-concept study investigates the potential of ILs to enhance transcorneal permeation of BBR for experimental AMD treatment *via* topical eye-drop administration.

We synthesized ILs using monoethanolamine (Mea) paired with biocompatible short-chain acids, malic (Ma), citric (Ci), and lactic acid (La) [16,22–24], selected based on their Generally Recognized as Safe (GRAS) status and documented superiority over long-chain analogs (*e.g.*, geranic acid) in safety and permeation-enhancing efficacy [16]. The rational design leveraged Mea's role as an essential animal nutrient and the favorable regulatory profiles of the organic acids, yielding three high-biocompatibility ILs, [Mea][Ci], [Mea][Ma], and [Mea][La].

While ILs show potential as carriers for BBR delivery, preliminary studies revealed a critical limitation: the high viscosity of ILs significantly impedes BBR release when formulated as a combined delivery matrix (one-step strategy) [16,22]. To overcome this challenge, we adopted a sequential two-step approach. This strategy first involves cornea surface pretreatment with ILs to permeabilize the cornea epithelium, followed by topic administration of BBR solution. Fig. 1 shows a schematic illustration of the rationale of a two-step *vs.* a one-step strategy. Notably, this sequential methodology has been successfully implemented in transdermal delivery systems [16,20].

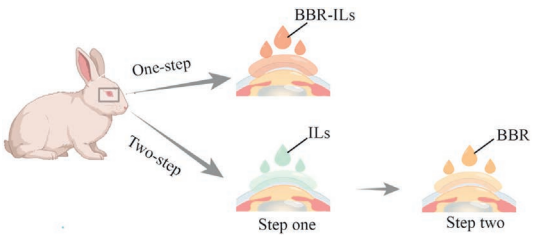


Fig. 1. Schematic illustration of the rationale of a two-step strategy versus a one-step strategy.

The ILs were synthesized following established protocols [16,24,25]. All resulting ILs appeared as viscous, colorless-to-yellowish liquids exhibiting moderate flowability (Fig. 2). The water content of all three ILs remained below 10 %. The pH values (7.0–7.7) fell within the acceptable range for ophthalmic preparations. Furthermore, all ILs maintained physical integrity without phase separation or precipitation after 48-h storage at room temperature, confirming physical stability. For more detailed operational methods, please refer to the Supporting information.

Nuclear magnetic resonance (NMR) analysis was conducted to characterize the three ILs and their reactants (Figs. 2A–G). The methylene signals of Mea (400 MHz, DMSO-*d*6) were observed at δ 3.33 (t, $J = 5.8$ Hz, 2H) (1,2) and 2.55 (t, $J = 5.8$ Hz, 2H) (3,4). Upon IL formation, these signals shifted downfield to δ 3.52-3.47 (m, 2H, H-1′,2′) and δ 2.75-2.70 (m, 2H, H-3′,4′). Concurrently, protons on the carboxyl-attached methyl or methylene groups of Ac, Ci, and La exhibited characteristic shifts. The carboxyl signals originating from Ac, Ci, and La were at δ 11.97 (s, 1H), δ 12.39 (s, 2H), and δ 12.5 (s, 1H), respectively. However, these signals disappeared post-reaction, confirming carboxyl-amino group condensation between the acids and Mea to form the target ILs.

Figs. 2H–J presents the Fourier transform infrared spectroscopy (FTIR) spectra of Mea-ILs. The spectrum of free Mea displayed characteristic N-H stretching vibrations (2800–3500 cm^{-1}) for primary amines. These peaks disappeared in all Mea-IL spectra, confirming amino group protonation *via* acid-base metathesis. Similarly, the carbonyl stretching band (~1760 cm^{-1}) of free acids vanished in corresponding ILs, replaced by carboxylate asymmetric stretches at 1550–1640 cm^{-1}, verifying anion formation. Figs. 2K–M illustrates water content effects on Mea-IL properties. pH values (Fig. 2K) initially rose then declined with increasing water content. [Mea][Ci] and [Mea][Ac] exhibited pronounced pH changes, while [Mea][La] remained stable, likely due to disrupted ionic networks enhancing ion dissociation at higher water content. Viscosity (Fig. 2L) inversely correlated with water content, with [Mea][Ci] exhibited the most significant change in viscosity, whereas the viscosities of [Mea][Ac] and [Mea][La] varied more gradually. Fig. 2M illustrated the relationship between the surface tension and water content of Mea-ILs. The surface tension of [Mea][Ci] gradually increased as the water content decreased, whereas the surface tension of [Mea][Ac] and [Mea][La] gradually decreased with decreasing water content.

To minimize ocular irritation, the pH values of all three ILs were maintained at 7.03–7.11, consistent with ophthalmic standards. Given the aqueous humor's role as the primary conduit for drug transit from the anterior to the posterior segments, we monitored the BBR levels in aqueous humors in rabbit models. Analysis revealed that permeability enhancement increased with IL exposure time (Fig. 3A), but irritation escalated beyond 15 min. Consequently, 10-min pretreatment was selected for subsequent studies. Among the ILs studied, [Mea][Ci] demonstrated superior permeation enhancement, likely attributable to Ci's higher carboxyl group density compared to Ma or La, as carboxyl moieties are primary determinants of IL permeation effects [23]. Building on prior findings that water content disrupts IL network interactions and compromises permeation [24], we examined the impact of the water content in [Mea][Ci] on permeation enhancement (Fig. 3B). Maximum efficacy occurred at <10 % water content.

The pharmacokinetic profile serves as a key indicator of [Mea][Ci]'s ability to enhance BBR penetration across ocular barriers. Comparative pharmacokinetic analysis in rabbit models revealed substantial differences between [Mea][Ci] and normal saline (NS) treatments (Fig. 3C and Table 1). This study has received approval from the Experimental Animal Ethics Committee of Fudan

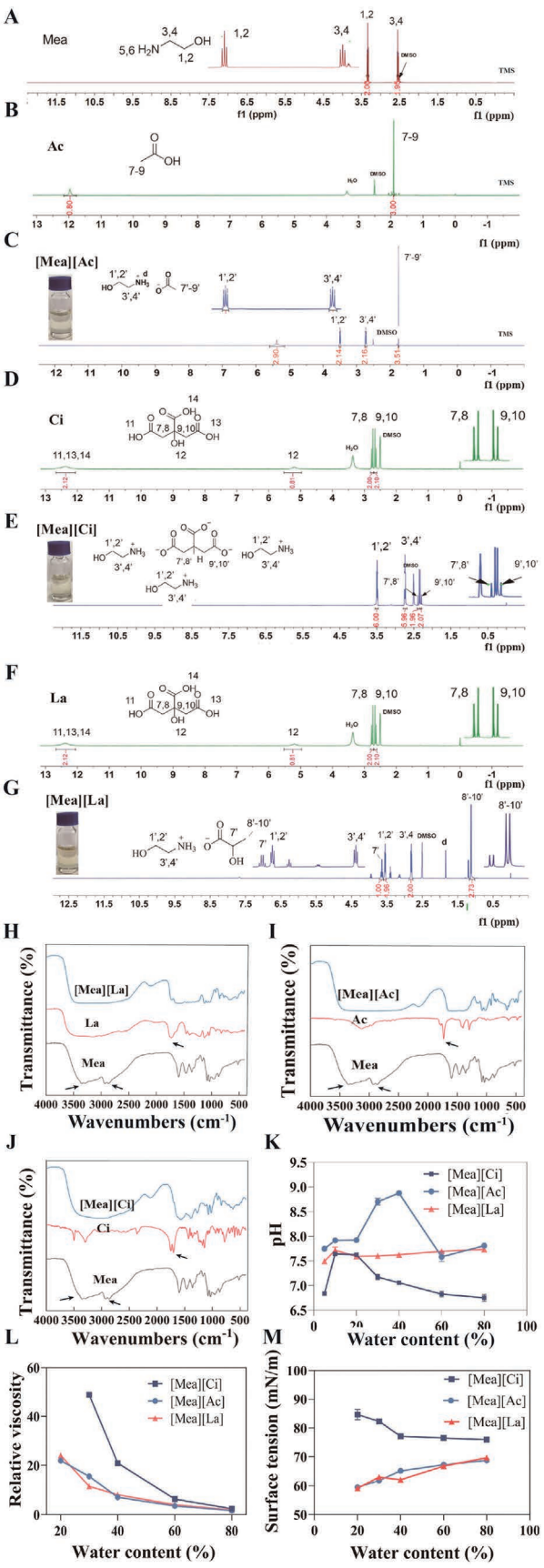


Fig. 2. ^{1}H-NMR spectra of Mea (A), Ci (B), [Mea][Ci] (C), Ac (D), [Mea][Ac] (E), La (F), and [Mea][La] (G). (H–J) Infrared spectroscopy (IR) spectra of Mea-ILs. (K–M) influence of water content in MEA-ILs on pH value, viscosity, and surface tension. Data are presented as mean ± standard deviation (SD) ($n = 3$).

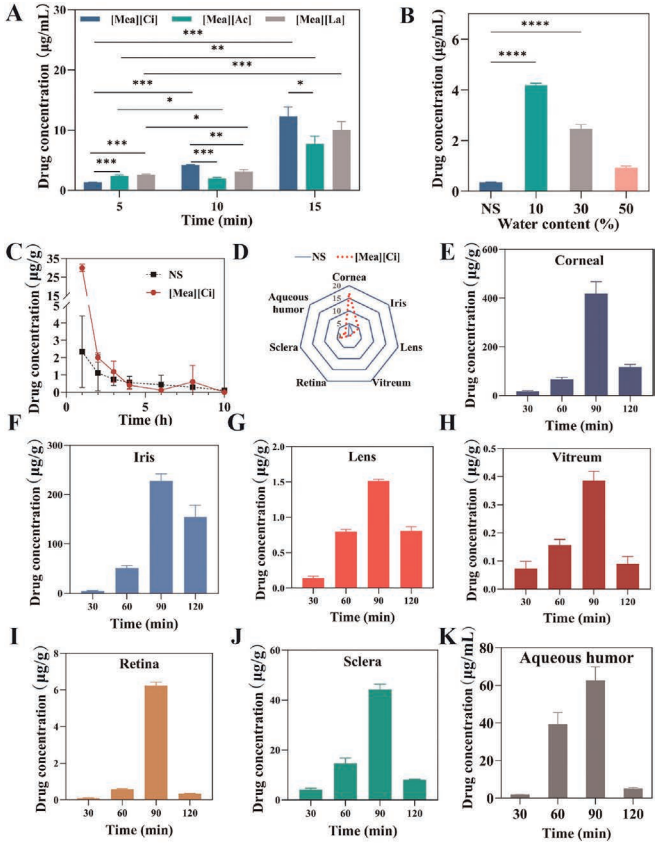


Fig. 3. (A, B) Impact of treatment duration and water content of ILs on the permeability enhancement mediated by Mea-ILs. (C) Pharmacokinetic profile of BBR in the intraocular aqueous humor following [Mea][Ci] treatment (mean ± SD, $n = 6$). (D) Tissue distribution of BBR in the NS group and [Mea][Ci] group 30 min after administration. (E–K) Tissue distribution of BBR in the eye in the [Mea][Ci] group (μg/g). NS: normal saline group. $^{*}P < 0.05$, $^{**}P < 0.01$, $^{***}P < 0.001$, $^{****}P < 0.0001$.

Table 1
Ocular pharmacokinetic parameters (mean ± SD, $n = 6$).

Group	NS	[Mea][Ci]
$T_{1/2}$ (h)	5.22 ± 3.86	0.93 ± 0.10
T_{max} (h)	1.00 ± 0.00	1.00 ± 0.00
C_{max} (μg/mL)	2.62 ± 1.73	29.92 ± 1.98
$AUC_{0-\infty}$ (μg mL^{-1} h)	6.90 ± 3.93	34.02 ± 2.44
AUC_{0-t} (μg mL^{-1} h)	5.28 ± 4.37	33.85 ± 2.43
MRT_{0-t} (h)	2.57 ± 1.12	1.20 ± 0.06

University School of Pharmacy (approval No. 202404009S). Notably, the $AUC_{0-\infty}$ of the [Mea][Ci] group was 4.93 times greater and the C_{max} was 11.42 times greater than that of the NS group ($P < 0.05$), respectively. The half-life ($T_{1/2}$) was determined to be 0.93 ± 0.1 h. These findings underscore [Mea][Ci]'s efficacy in modulating corneal barrier function to significantly boost BBR absorption without prolonging ocular residence time. Further tissue distribution analysis showed markedly different spatial-temporal patterns. At 30 min post-administration, the NS group presented minimal BBR levels across all ocular tissues (Fig. 3D), whereas [Mea][Ci] pretreatment enabled detectable BBR levels throughout the eye. Subsequent time-course evaluation (60–120 min) revealed peak BBR concentrations in most ocular tissues at 90 min followed by gradual decline, though sustained levels persisted beyond 120 min in the cornea, iris, and sclera. Notably, posterior segment penetration remained limited, with lens and vitreous concentrations reaching only 1.5 and 0.41 μg/g respectively at 90 min.

Ocular irritation assessment represents a critical safety benchmark for ophthalmic formulations, as irritation can induce ex-

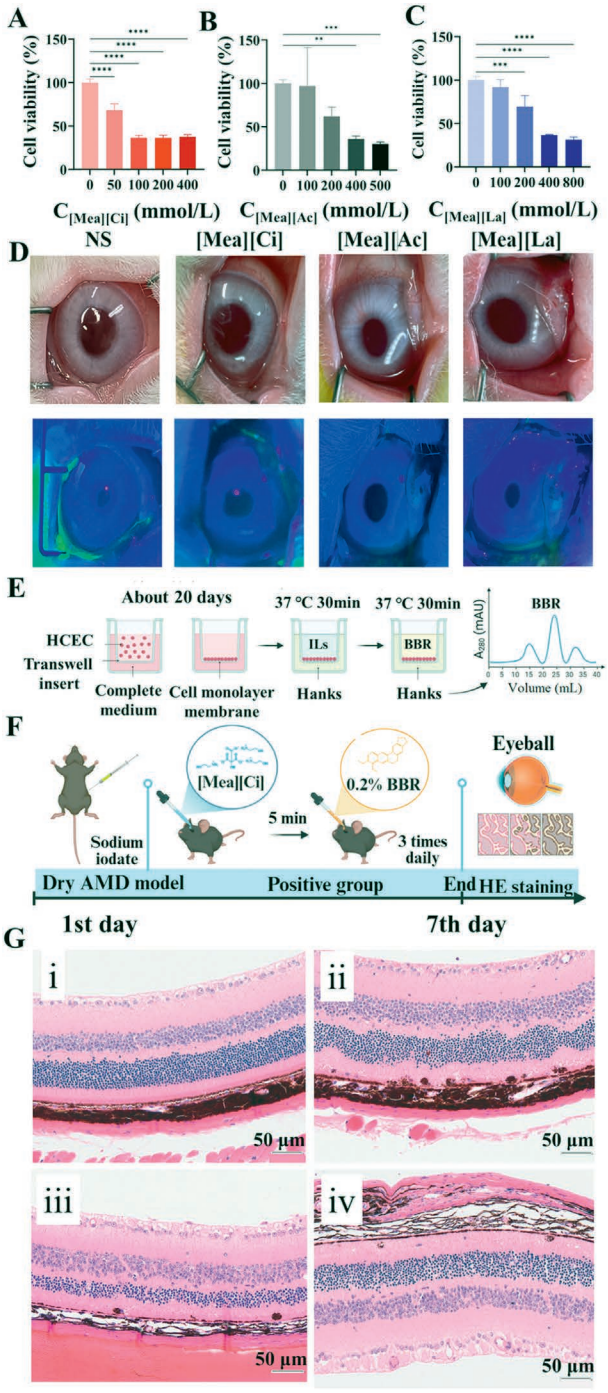


Fig. 4. (A–C) Cytotoxicity of Mea-IL mixture. Data are presented as mean ± SD ($n = 4$). (D) Eye irritation test results. The upper row: examination under daylight; the lower row: examination under cobalt blue light after the application of fluorescein sodium. (E) Investigation of the ability of Mea-IL to promote BBR transmembrane transport. Created at BioRender.com. (F) Treatment methods for positive groups in efficacy trials. (G) Histopathological changes in mouse retinal tissue stained with HE after 7 days of drug administration (i. normal saline group; ii. model group; iii. negative control group; iv. positive control group). Scale bar: 50 μm. NS: normal saline group. $^{**}P < 0.01$, $^{***}P < 0.001$, $^{****}P < 0.0001$.

cessive lacrimation, compromise ocular surface integrity, and ultimately impair drug efficacy. Additionally, it poses toxic risks to ocular cells including corneal and retinal pigment epithelia. We adopted HCECs cells to assess the cytotoxicity of Mea-ILs following 2-h exposure (Figs. 4A–C) [26]. The results revealed half maximal inhibitory concentration (IC_{50}) values of 94.1, 356.6, and 367.7 mmol/L for [Mea][Ci], [Mea][Ac], and [Mea][La], respectively. In comparison, the IC_{50} of benzalkonium bromide, a commonly utilized penetration enhancer on the market [12], is 0.033 mmol/L, indicating a significant increase in safety with Mea-ILs. The concentrations of the three ILs required to maintain the survival of 80% of HCECs were 1169.1, 915.7, and 934.8 mmol/L, indicating their safety as ocular penetration enhancers. A previous study on L-carnitine- and betaine-based ILs reported excellent ocular tolerance and safety in rabbit eyes with IC_{50} values of 26.8 and 27.8 mmol/L against HCEC cell lines, respectively [18], which are 3–10 times more toxic than those of the Mea-ILs. Draize testing (Fig. 4D) revealed only mild transient conjunctival hyperemia upon initial application, which diminished with continued use. After 7-day exposure, minimal mucus secretion was observed without corneal epithelial damage, confirmed by absent fluorescein sodium pooling under cobalt blue light examination.

While the precise mechanisms by which ILs enhance corneal permeability remain incompletely understood, two principal pathways have been identified. First, ILs significantly increase drug solubility in ocular media, establishing a prerequisite for membrane permeation. Second, they modulate membrane lipid fluidity and hydrophilic/hydrophobic balance, thereby enhancing membrane permeability [27]. Transcorneal transport studies quantified this enhancement *via* apparent permeability coefficient (P_{app}). Treatment with Mea-ILs significantly increased P_{app} values in HCEC monolayers (Fig. 4E): [Mea][Ac] = 0.404 ± 0.144 cm/h, [Mea][Ci] = 0.254 ± 0.034 cm/h, and [Mea][La] = 0.240 ± 0.069 cm/h. Notably, these values remained substantially lower than cell-free controls (1.898 ± 0.122) cm/h, confirming that ILs enhance permeability without inducing cytotoxic membrane disruption. These P_{app} values represent a >50-fold increase over baseline BBR permeability in rabbit corneas (4.998×10^{-3} cm/h) [7], demonstrating ILs' remarkable permeation-enhancing capacity.

Several animal models exist for studying dry AMD, including the sodium iodate injection model [28,29], cigarette smoke exposure model [30], and blue light irradiation model [28]. Among these, intraperitoneal injection of sodium iodate stands out as a relatively well-established approach for inducing a dry AMD phenotype. This model induces retinal oxidative damage characterized primarily by RPE cell necrosis, choroidal capillaries atrophy, and retinal morphological alterations [31]. These changes ultimately lead to apoptosis and reduced cell counts in the RPE and outer nuclear layer (ONL), among other retinal cells. In this study, we established a dry AMD model *via* intraperitoneal sodium iodate injection (Fig. 4F). Subsequently, retinal pathological changes were assessed using hematoxylin-eosin (HE) staining seven days post-injection (Fig. 4G). Normal mouse retinas exhibited intact architecture, with nearly spherical ONL nuclei uniformly and compactly arranged in distinct layers (Fig. 4G(i)). These nuclei were enclosed by a thin stromal membrane, effectively isolating them from the cytoplasm. In contrast, the sodium iodate-induced model group displayed progressive disorganization, including loosening of cellular arrangement, regional ONL thinning, and nuclear deformation. In particular, severe structural distortions were observed in specific areas of both the inner nuclear layers (INL) and ONL (Fig. 4G(ii)). The negative control group showed minor retinal alterations, featuring localized layer disorganization and focal ONL attenuation. Conversely, the positive control group (BBR-treated) exhibited minimal retinal alterations without electrocardiogram-like alterations, maintaining well-organized laminar structure (Fig. 4G(iii)). A marked morphological distinction was evident between these groups (Fig. 4G(iv)), demonstrating BBR's superior therapeutic efficacy over untreated controls in the dry AMD model. HE staining results indicate that BBR's antioxidant properties effectively reversed sodium iodate-induced retinal deformation, demonstrating therapeutic benefit for dry AMD. Critically, while healthy retinas remained intact, the model group showed severe INL/ONL distor-

tion in specific regions. The negative control's minor changes with local disorganization contrasted sharply with the positive control's well-preserved retinal architecture, highlighting BBR's potent antioxidative stress effects.

This study significantly expands the application of ILs in ocular drug delivery, proposing a safe and efficient novel approach for BBR in treating dry AMD. It also represents the first investigation into the use of Mea-ILs as penetration enhancers for ocular drug delivery, including comprehensive analysis of their penetration-enhancing capabilities, ocular biocompatibility, and therapeutic efficacy. Furthermore, this work provides a foundational reference for the future development and application of ILs as penetration enhancers in noninvasive posterior segment drug delivery.

Declaration of competing interest

The authors declare that they have no known competing financial interests or personal relationships that could have appeared to influence the work reported in this paper.

CRediT authorship contribution statement

Xiuyan Li: Writing – original draft, Visualization, Methodology, Investigation, Funding acquisition, Formal analysis. **Chongjiang Wang:** Methodology, Investigation, Data curation. **Xiwu Zhang:** Validation, Investigation, Formal analysis. **Chengcheng Zhao:** Methodology, Investigation. **Zhihui Yang:** Validation, Resources. **Yi Lu:** Resources, Project administration. **Yifan Cai:** Investigation, Data curation. **Huiping Lu:** Resources. **Hailong Yuan:** Writing – review & editing, Supervision, Resources, Conceptualization. **Wei Wu:** Writing – review & editing, Supervision, Resources, Project administration, Conceptualization. **Yikang Dai:** Writing – review & editing, Resources, Project administration, Methodology, Investigation, Formal analysis, Conceptualization.

Acknowledgments

This work was supported by the Heilongjiang Provincial Administration of Traditional Chinese Medicine (No. ZHY2020-93). The "Unveiling the List and Taking the Helm" Project of Heilongjiang Province (No. 2023ZXJ02C02), the "Excellent Young Teachers' Basic Research Support Program" of Heilongjiang Province (No. YQJH2023150), and the Scientific Research Project of Heilongjiang University of Chinese Medicine (No. 2019JC01) were included.

Supplementary materials

Supplementary material associated with this article can be found, in the online version, at doi:10.1016/j.cclet.2025.111714.

References

[1] A. Stahl, Dtsch. Arztebl. Int. 117 (2020) 513–520.
[2] W.L. Wong, X. Su, X. Li, et al., Lancet Glob. Health 2 (2014) e106–e116.
[3] T.A. Cabral De Guimaraes, M.Daich Varela, M. Georgiou, et al., Br. J. Ophthalmol. 106 (2022) 297–304.
[4] D. Song, J. Hao, D. Fan, Front. Med. 14 (2020) 564–582.
[5] Q. Chen, Phytomedicine 104 (2022) 154181.
[6] S. Li, U. Gaur, C.M. Chong, et al., Int. J. Mol. Sci. 19 (2018) 1736.
[7] F. Li, Preparation and Effects of Berberine hydrochloride Nanoemulsion on Mouse Model of dry AMD, Dissertation, Jiangxi University of Chinese Medicine, Nanchang, 2024.
[8] S. Lai, Y. Wei, Q. Wu, et al., J. Nanobiotechnology 17 (2019) 64.
[9] C. Huang, Z. Zhang, J. Gu, et al., Int. J. Nanomedicine 18 (2023) 4347–4363.
[10] N. Alsabeelah, V. Kumar, J. Food Biochem. 46 (2022) e14361.
[11] M. Reibaldi, T. Avitabile, F. Bandello, et al., J. Clin. Med. 8 (2019) 1031.
[12] X. Chen, Z. Li, C. Yang, et al., Asian J. Pharm. Sci. 19 (2024) 100900.
[13] E. Beaven, R. Kumar, J.M. An, et al., Adv. Drug Deliv. Rev. 204 (2024) 115157.
[14] Y. Lu, Y. Ma, W. Wu, MedComm Biomater. Appl. 3 (2024) e81.
[15] L. Zhang, Z. Dong, S. Yu, et al., Chin. Chem. Lett. 35 (2024) 109101.
[16] Y. Li, Q. Yu, Y. Lu, et al., Int. J. Pharm. 667 (2024) 125006.
[17] B. Xie, Q. Jiang, F. Zhu, et al., Chin. Chem. Lett. 36 (2025) 110508.
[18] B. Grassiri, A. Mezzetta, G. Maisetta, et al., Int. J. Mol. Sci. 24 (2023) 2714.
[19] J. Wang, B. Li, J. Tang, et al., ACS Pharmacol. Transl. Sci. 5 (2022) 752–760.
[20] Q. Yu, X. Wu, Y. Lu, et al., ACS Appl. Bio Mater. 7 (2024) 2899–2910.
[21] Y. Li, X. Wu, Q. Zhu, et al., Int. J. Pharm. 569 (2019) 118584.
[22] Y. Li, Q. Yu, Y. Lu, et al., Drug Deliv. Transl. Res. 15 (2025) 1693–1706.
[23] X. Wu, Z. Chen, Y. Li, et al., Int. J. Pharm. 558 (2019) 380–387.
[24] X. Wu, J. Xuan, Q. Yu, et al., Pharm. Res. 39 (2022) 2421–2430.
[25] K. Liu, W. Liu, Z. Dong, et al., Bioeng. Transl. Med. 8 (2023) e10405.
[26] K.B. Wróblewska, B. Milanowski, M. Kucińska, et al., Pharmaceuticals 14 (2021) 849.
[27] Q.M. Qi, S. Mitragotri, J. Control. Release (2019) 162–169 311-312.
[28] S. Reichl, C. Kölln, M. Hahne, et al., Expert Opin. Drug Metab. Toxicol. 7 (2011) 559–578.
[29] S. Reichl, J. Pharm. Pharmacol. 60 (2008) 299–307.
[30] S. Dey, Expert Opin. Drug Metab. Toxicol. 7 (2011) 529–532.
[31] D. Song, J. Song, C. Wang, et al., Exp. Eye Res. 145 (2016) 1–9.